Science Bulletin xxx (xxxx) xxx

Contents lists available at ScienceDirect

Science Bulletin

journal homepage: www.elsevier.com/locate/scib

Short Communication

π-π stacking constructing efficient charge channels for perovskite photovoltaics

Chun-Hao Chen [a,1], Fan Hu [a,1], Kai-Li Wang [a], Jing Chen [a], Tian-Yu Teng [a], Yi-Ran Shi [a], Yu Xia [a], Zhen-Huang Su [b], Xing-Yu Gao [b], Ilhan Yavuz [c], Zhao-Kui Wang [a,*], Liang-Sheng Liao [a]

[a] Institute of Functional Nano & Soft Materials (FUNSOM), Jiangsu Key Laboratory of Advanced Negative Carbon Technologies, Jiangsu Key Laboratory for Carbon-Based Functional Materials & Devices, Soochow University, Suzhou 215123, China
[b] Shanghai Synchrotron Radiation Facility, Shanghai Advanced Research Institute, Shanghai Institute of Applied Physics, Chinese Academy of Sciences, Shanghai 201204, China
[c] Department of Physics, Marmara University, Istanbul 34722, Turkey

ARTICLE INFO

Article history:
Received 20 September 2023
Received in revised form 2 November 2023
Accepted 21 November 2023
Available online xxxx

Perovskite solar cells (PSCs) have emerged as strong potential candidates for future photovoltaic technologies. The power conversion efficiency (PCE) of PSCs has already surpassed 26%, approaching their theoretical limit [1]. The commonly used device structure for PSCs is ITO/SnO_2/perovskite/2,2′,7,7′-tetrakis-(*N*,*N*-di-4-methoxyphenylamino)-9,9′-spirobifluorene (spiro-OMeTAD)/Au [2]. Among various strategies to optimize device performance, the most promising one involves interface engineering for the perovskite thin film. Typically, organic ammonium salts can passivate defects in the perovskite thin film, effectively enhancing device efficiency [3]. Optimizing the band edges at the perovskite surface and matching the interface energy levels can improve the open-circuit voltage of the device [3,4]. Additionally, a water-resistant barrier layer can effectively isolate water vapor and suppress lead leakage, thus improving device stability and safety [5]. These mature and effective strategies primarily focus on the interaction between interface optimization molecules and the perovskite layer. However, these strategies take little account of the interaction between the interface molecules and the upper-hole transport layer, spiro-OMeTAD.

The interaction between the interface molecules and the hole transport layer can effectively improve the hole mobility and match the interface energy level [6]. In this study, for the first time, we thoroughly explored the π-π stacking interactions between the interface modification layer and hole transport layer, investigating their impact on charge carrier transport. In detail, 2-(naphthyl-2-yl) ethylamine hydroiodic acid salt (NEAI) was opted as the interface optimization molecules, which is a kind of typical condensed nucleus compound with the common primary ammonium passivating groups [3]. The intermolecular interactions include edge-to-face CH-π interactions and face-to-face π-π stacking, with the latter being beneficial for charge carrier transport in their channels [7]. Through density functional theory (DFT) calculations, we found that the π-π interaction between the naphthalene ring in NEAI and spiro-OMeTAD is stronger than that of phenylethylamine iodide (PEAI) and ethylamine hydroiodate (EAI) [8]. The stronger binding energy improves the extraction and transport of charge carriers, thereby enhancing the short-circuit current density of PSCs. Furthermore, NEAI interface engineering enables the formation of a layer of 2D phase with n = 1 at the perovskite surface, leading to the construction of a 2D/3D perovskite heterojunction structure. The 2D perovskite layer reduces the density of surface defect states, decreases non-radiative recombination, and thereby improves the open-circuit voltage of the device [9].

EAI-treated perovskite was considered as the pristine group, which possesses a basic tertiary ammonium group. PEAI and NEAI were compared and analyzed as experimental groups. Firstly, DFT calculations were employed to elucidate the interaction patterns and structures between PEAI, NEAI, and spiro-OMeTAD. We observed two types of intermolecular interactions: CH-π (Fig. S1 online) and π-π. Due to extended orbital delocalization of a condensed ring like the naphthalene, their intermolecular interactions exhibited stronger binding energies compared with the benzene ring. The effectiveness of CH-π interactions in charge carrier transport is an order of magnitude lower than that of π-π interactions [10]. We further calculated the structures and binding energies under π-π interactions as shown in Fig. 1a. The face-to-face distances between the benzene rings in PEAI and spiro-OMeTAD were calculated as 3.48 Å, while the corresponding distance between NEAI and spiro-OMeTAD was 3.72 Å, implying a similar magnitude.

* Corresponding author.
E-mail address: zkwang@suda.edu.cn (Z.-K. Wang).
[1] These authors contributed equally to this work.

https://doi.org/10.1016/j.scib.2023.11.052

Please cite this article as: C.-H. Chen, F. Hu, K.-L. Wang et al., π-π stacking constructing efficient charge channels for perovskite photovoltaics, Science Bulletin, https://doi.org/10.1016/j.scib.2023.11.052

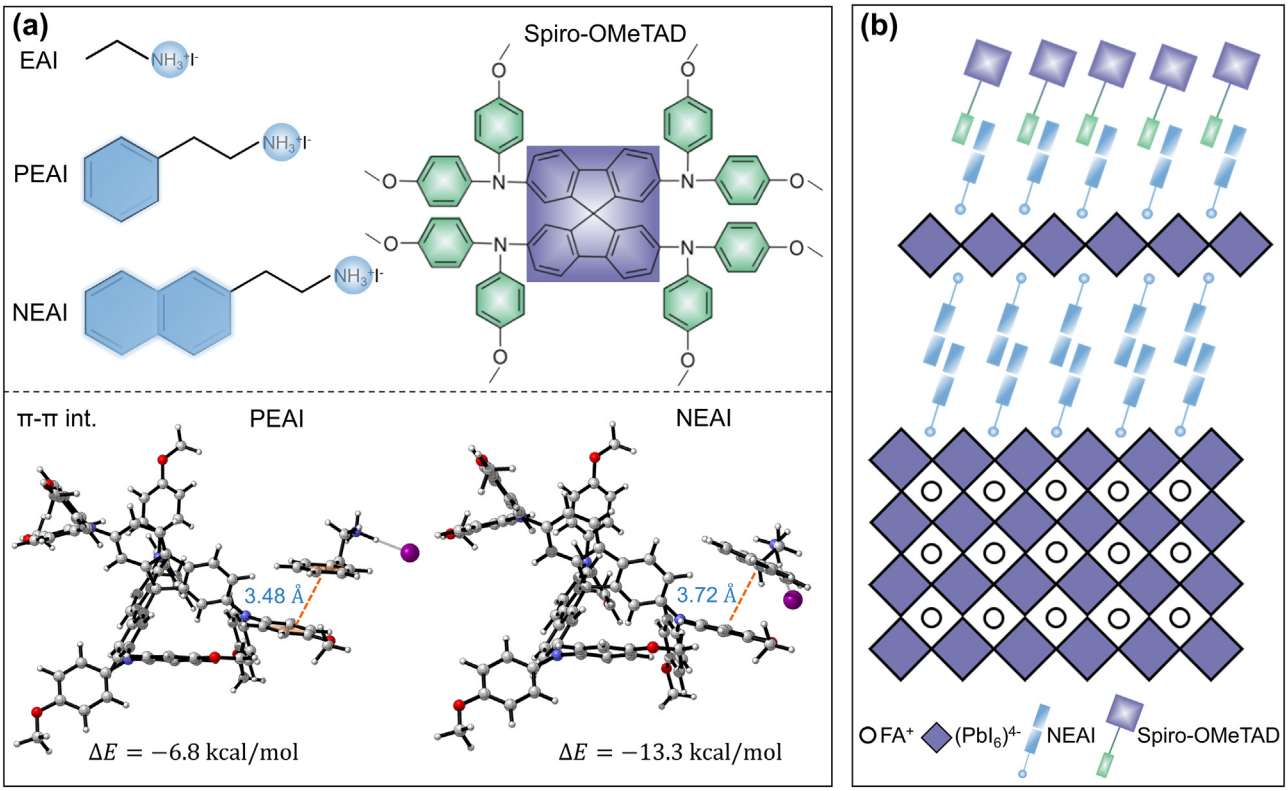

Fig. 1. (Color online) DFT calculations of π-π interaction between NEAI and spiro-OMeTAD. (a) Chemical structure diagram of EAI, PEAI, NEAI, and spiro-OMeTAD, and DFT calculations of π-π interaction between PEAI/NEAI and spiro-OMeTAD. (b) Schematic of perovskite surface after NEAI treatment.

However, the binding energy between NEAI and spiro-OMeTAD reached −13.3 kcal/mol, approximately twice that of PEAI and spiro-OMeTAD (−6.8 kcal/mol), which has the opposite trend with the face-to-face distance. We further validated the performance modification effect of NEAI compared with PEAI using comprehensive characterization. Fig. 1b illustrates the surface structure of the perovskite film after NEAI treatment. The ammonium group fills the A-site on the perovskite surface, while the naphthalene group at the other end exhibits a face-to-face π-π stacking with the benzene ring in spiro-OMeTAD. Additionally, through the grazing incidence X-ray diffraction (GIXRD) characterization, we observed the formation of a distinct 2D perovskite phase with $n = 1$ on the NEAI-treated surface, enabling the construction of a surface heterojunction in perovskite.

Then we further validate the existence of π-π interactions. The X-ray photoelectron spectroscopy (XPS) C 1s analysis was performed on spiro-OMeTAD films doped with EAI, PEAI, and NEAI with the same concentration of 0.1 M (1 M = 1 mol/L) (Fig. S2 online). We fitted the spectra of the three films and observed a π-π* satellite peak at a binding energy of approximately 290.9 eV [11]. In the case of spiro-OMeTAD doped with EAI, this peak is attributed to the intrinsic π system between the benzene rings of spiro-OMeTAD itself [12]. The fitting area of this peak accounted for 1.66% of the total (Table S1 online). However, the fitting areas of the peaks corresponding to the π system in spiro-OMeTAD films doped with PEAI and NEAI were increased compared with the original EAI-doped films, reaching 2.52% and 4.83%, respectively. Furthermore, ^{1}H nuclear magnetic resonance (NMR) tests were performed on spiro-OMeTAD solutions doped with EAI, PEAI, and different concentrations of NEAI (Fig. S3 online). There are no significant chemical shift changes in the EAI-doped samples. We observed a chemical shift towards higher field values in the peaks corresponding to the conjugated structure of the spiro-OMeTAD benzene rings, where the fluorene and arylamine core peaks were located around 6.9 and 6.75 ppm, as NEAI doping increased. Therefore, this further confirms the presence of π-π interactions between spiro-OMeTAD and NEAI. In addition, due to the weaker π-π interaction between the PEAI and spiro-OMeTAD than that of NEAI, the chemical shift is relatively smaller.

J–V measurements on PSCs with surface treatments of EAI (pristine) and NEAI (target) showed an improvement in J_{SC} due to the π-π interactions between NEAI and spiro-OMeTAD. The average J_{SC} increased from 25.2 mA/cm^2 in the pristine device to 26.2 mA/cm^2 in the target device as shown in Fig. S4 (online). The average J_{SC} of PEAI-treated devices is 25.45 mA/cm^2, which is slightly higher than the original device. J_{ph}–V_{eff} curves were plotted to investigate charge collection and exciton dissociation (Fig. S5 online) [13]. The J_{ph}/J_{sat} ratio of EAI treated original device and NEAI treated optimized device is 0.973 and 0.985, respectively under short circuit conditions. The ratio of the target device is larger, which indicates that the charge collection and extraction effect is better. It is proven that the π-π interaction between naphthalene ring and spiro-OMeTAD is conducive to carrier transport. Further, we studied the effect of NEAI interface treatment on the hole mobility of perovskite by using the space-charge-limited current (SCLC) model (Fig. S6 online). The mobility was increased from the original 1.8×10^{-4} to 4.4×10^{-4} cm^2 V^{-1} s^{-1} after treatment. In addition, time-resolved photoluminescent (TRPL) (Fig. S7 online) proves that the existence of π-π interaction is conducive to the interfacial transport of carriers.

Furthermore, through cross-section scanning electron microscopy (SEM) tests, we observed excellent crystalline quality of the perovskite film with uniform and large grain sizes (Fig. S8 online). Compared with the pristine film, the NEAI-optimized film exhibited superior surface connectivity and smoothness on the perovskite layer. The photoluminescence (PL) mapping test was

conducted on the perovskite film as shown in Figs. S9 and S10 (structure: ITO/SnO_2/perovskite/spiro-OMeTAD). The target film exhibited relatively weaker and more uniform PL intensity [14]. Furthermore, the intensity of the conductive atomic force microscopy (CAFM) (Fig. S11 online) increased from the original 252 pA to the target 326 pA (Fig. S12, Fig. S13 online). This directly indicates the improvement of hole extraction efficiency in spiro-OMeTAD due to the NEAI treatment. The AFM 3D topography as shown in Fig. S14 (online) demonstrates better surface flatness of the optimized perovskite films.

To further validate the crystalline effects of different materials on the surface treatment, GIXRD analysis was conducted on the perovskite films (Fig. S15 online). Specifically, we found a strong (020) peak of the n = 1 two-dimensional phase in the NEAI surface-treated perovskite film at q = 4 nm^{-1}, which was almost absent in the EAI-treated films and not obvious in PEAI-treated films. As shown in Fig. 1b, NEA^+ acts as the R-site in the two-dimensional phase, forming an ordered n = 1 phase on the surface [15]. The formation of the two-dimensional phase enabled the construction of a 2D/3D perovskite heterojunction, which reduced the density of surface defect states, minimized non-radiative recombination in the perovskite absorber layer, and thereby improved the open-circuit voltage of the devices. The peak wavelength of the perovskite PL (Fig. S16 online) shifted from 812 to 807 nm, that is, the bandgap increased from 1.53 to 1.54 eV, which confirmed that the NEAI treatment altered the band edges and formed a 2D/3D perovskite heterojunction [4]. The increase in PL intensity indicated a reduction in non-radiative recombination which is also consistent with the results in PL mapping as shown in Fig. S17 (online). The TRPL spectra of the perovskite films (structure: ITO/Perovskite) in Fig. S18 (online) showed that the target perovskite film displayed a longer lifetime, increasing from the original 232 to 414 ns. The PEAI treated perovskite film showed a lifetime of 295 ns. The NEAI treatment formed a thin layer of two-dimensional phase on the surface, reducing non-radiative recombination and greatly extending the carrier lifetime. The treated films exhibited lower trap density of states (tDOS) (Fig. S19 online) in the shallow trap region of 0.3–0.35 eV and the deep trap region above 0.4 eV. This indicates a reduction in point defect and dangling bond density on the surface of the NEAI-treated perovskite films. The derived drive-level capacitance profiling (DLCP) curves through capacitance–voltage (C–V) measurements, as shown in Fig. S20 (online), revealed a significant reduction in trap density in the upper layer of the treated film.

Finally, the performance of the devices was tested. The J–V curves showed higher J_{SC} and V_{OC} in the optimized devices (Fig. 2a and Fig. S21 online). The performance parameters of the devices are listed in Table S2 (online) The original devices treated with EAI exhibited J_{SC} of 25.5 mA/cm^2, V_{OC} of 1.13 V, fill factor (FF) of 78.1%, and PCE of 22.57%. The devices treated with PEAI displayed J_{SC} of 26.1 mA/cm^2, V_{OC} of 1.16 V, FF of 80.2%, and PCE of 24.32%. After optimization with NEAI, the devices showed J_{SC} of 26.4 mA/cm^2, V_{OC} of 1.18 V, FF of 80.3%, and PCE of 25.04%. The external quantum efficiency (EQE) of the optimized devices, as shown in Fig. 2b, had an integrated J_{SC} of 25.64%, which closely matched the actual J_{SC}. In addition, the optimized device exhibited negligible hysteresis (Fig. S22 online). The PCE distribution followed a Gaussian distribution and the average PCE improved from the original 22.09% to 24.49% (Fig. 2c). The PEAI treated devices showed an average PCE of 23.25% (Fig. S23 online). Fig. 2d displayed the J_{SC} and PCE measured at the maximum power point (MPP) within 3 min. The PCE increased from 21.78% to 24.27% after optimization with better output stability. Importantly, the stability of the devices significantly improved (Fig. 2e and Fig. S24 online) because of the lower trap density of states of the optimized perovskite films. After 1000 h of tracking tests, the PCE of the optimized devices remained at 94.5%, significantly higher than the original devices (70.4%) and the PEAI-treated ones (85.8%).

In summary, for the first time, we thoroughly explored the π-π stacking interactions between the interface modification layer and hole transport layer, investigating their impact on charge carrier transport optimization. NEAI interface engineering facilitates the formation of a 2D phase on the perovskite surface, creating a 2D/3D perovskite heterojunction structure. This work underscores

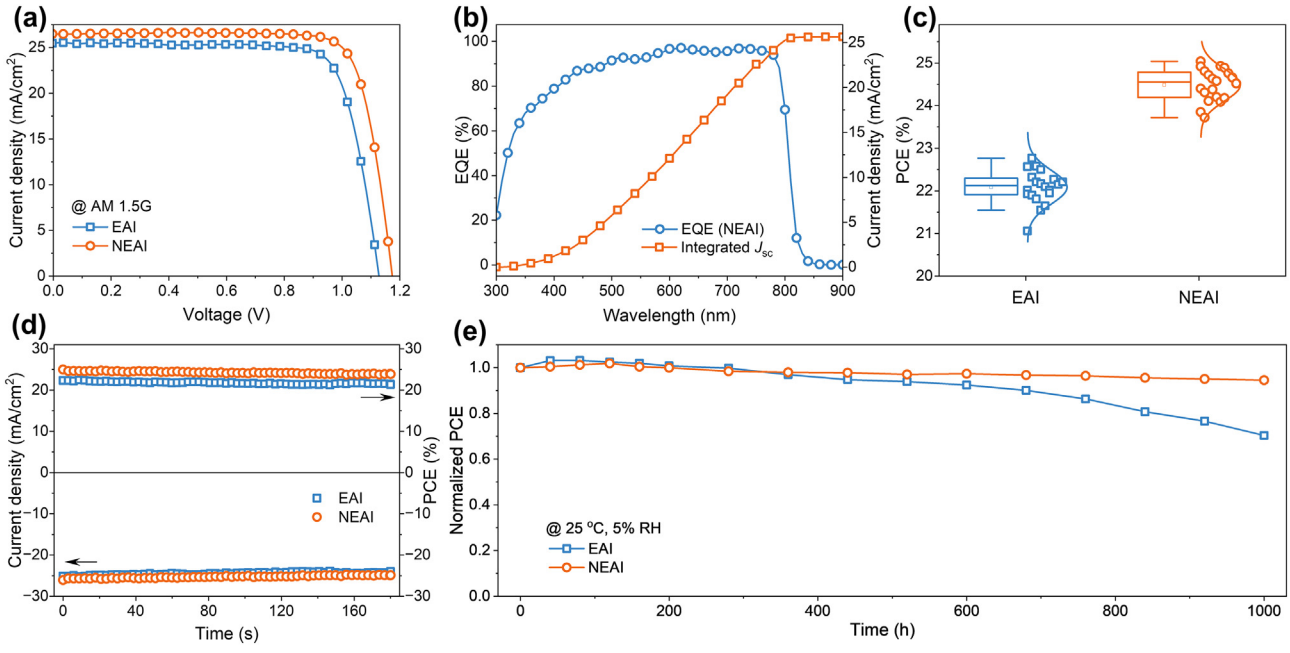

Fig. 2. (Color online) The performance of the perovskite photovoltaic devices. (a) The J–V curves under AM 1.5G. (b) EQE of the NEAI-treated PSCs and its integral current density. (c) The PCE distribution of 20 sets of devices for pristine and target PSCs. (d) Steady photocurrent and PCE at the maximum power output point within 3 min. (e) The PCE degradation curves.

the crucial role of π-π interactions and 2D/3D heterojunction engineering for high-performance perovskite photovoltaics. Ultimately, we achieve dual optimization of current and voltage, resulting in a champion PCE of 25.04%.

Conflict of interest

The authors declare that they have no conflict of interest.

Acknowledgments

The authors acknowledge financial support from the National Natural Science Foundation of China (52073197, 62075148, and 52273189), the Natural Science Foundation of Jiangsu Province (BZ2023052, BE20220262, and BK20211314), and Suzhou Science and Technology Plan Project (N321461821 and ST202212). The authors acknowledge Postgraduate Research & Practice Innovation Program of Jiangsu Province (23214000). The authors thank beamline BL14B1 at the Shanghai Synchrotron for providing the beam time. This work was supported by Suzhou Key Laboratory of Functional Nano & Soft Materials, Collaborative Innovation Center of Suzhou Nano Science & Technology, the 111 Project, Joint International Research Laboratory of Carbon-Based Functional Materials and Devices, and Soochow University Tang Scholar.

Author contributions

Chun-Hao Chen, Fan Hu, and Zhao-Kui Wang conceived the idea. Chun-Hao Chen fabricated the solar cell devices and designed the experiments. Zhen-Huang Su performed the GIXRD measurement under the supervision of Xing-Yu Gao. Ilhan Yavuz performed the DFT calculation. DFT calculations are performed in the UHEM computing cluster of Istanbul Technical University, Turkey. Fan Hu, Kai-Li Wang, Jing Chen, Tian-Yu Teng, Yi-Ran Shi, and Yu Xia assisted with the device fabrication and characterizations. Chun-Hao Chen, Zhao-Kui Wang, and Liang-Sheng Liao wrote the manuscript. All the authors discussed the results and commented on the manuscript. Zhao-Kui Wang and Liang-Sheng Liao supervised the project.

Appendix A. Supplementary materials

Supplementary materials to this short communication can be found online at https://doi.org/10.1016/j.scib.2023.11.052.

References

[1] NREL. Best Research-Cell Efficiency Chart, https://www.nrel.gov/pv/cell-efficiency.html (accessed June 30, 2023).
[2] Wang K, Li X, Lou Y, et al. $CsPbBrI_2$ perovskites with low energy loss for high-performance indoor and outdoor photovoltaics. Sci Bull 2021;66:347–53.
[3] Xue J, Wang R, Chen X, et al. Reconfiguring the band-edge states of photovoltaic perovskites by conjugated organic cations. Science 2021;371:636–40.
[4] Gharibzadeh S, Nejand B, Jakoby M, et al. Record open-circuit voltage wide-bandgap perovskite solar cells utilizing 2D/3D perovskite heterostructure. Adv Energy Mater 2019;9:1803699.
[5] Jiang Y, Qiu L, Juarez-Perez E, et al. Reduction of lead leakage from damaged lead halide perovskite solar modules using self-healing polymer-based encapsulation. Nat Energy 2019;4:585–93.
[6] Jung EH, Jeon NJ, Park EY, et al. Efficient, stable and scalable perovskite solar cells using poly(3-hexylthiophene). Nature 2019;567:511–5.
[7] Wang J, Huang H, Wang P, et al. Co-facial π-π interaction expedites sensitizer-to-catalyst electron transfer for high-performance CO_2 photoreduction. JACS Au 2022;2:1359–74.
[8] Zhang Y, Yuan S, Zhou W, et al. Spectroscopic evidence and molecular simulation investigation of the π-π interaction between pyrene molecules and carbon nanotubes. J Nanosci Nanotechnol 2007;7:2366–75.
[9] Zhang C, Wu S, Tao L, et al. Fabrication strategy for efficient 2D/3D perovskite solar cells enabled by diffusion passivation and strain compensation. Adv Energy Mater 2020;10:2002004.
[10] Feng A, Zhou Y, Al-Shebami M, et al. σ-σ Stacked supramolecular junctions. Nat Chem 2022;14:1158–64.
[11] Zeng L, Liu X, Chen X, et al. π-π Interaction between carbon fibre and epoxy resin for interface improvement in composites. Compos Part B-Eng 2021;220:108983.
[12] Choi Y, Koo D, Jeong M, et al. Toward all-vacuum-processable perovskite solar cells with high efficiency, stability, and scalability enabled by fluorinated spiro-OMeTAD through thermal evaporation. Sol RRL 2021;5:2100415.
[13] Xu M, Zhu X, Shi X. Plasmon resonance enhanced optical absorption in inverted polymer/fullerene solar cells with metal nanoparticle-doped solution-processable TiO_2 layer. ACS Appl Mater Interfaces 2013;5:2935–42.
[14] Dong Y, Shen W, Dong W, et al. Chlorobenzenesulfonic potassium salts as the efficient multifunctional passivator for the buried interface in regular perovskite solar cells. Adv Energy Mater 2022;12:2200417.
[15] Lei L, Seyitliyev D, Stuard S, et al. Efficient energy funneling in quasi-2D perovskites: from light emission to lasing. Adv Mater 2020;32:1906571.

Chun-Hao Chen is now a Ph.D. student of materials science and engineering under the supervision of Prof. Zhao-Kui Wang at Functional Nano & Soft Materials Laboratory of Soochow University, China. He received his B.S. degree at Soochow University in 2020. His research interest mainly focuses on environmentally friendly indoor flexible perovskites solar cells.

Fan Hu is now a master of Physics under the supervision of Prof. Zhao-Kui Wang at Functional Nano & Soft Materials Laboratory of Soochow University, China. He received his B.S. degree at Yanshan University in 2021. His research interest mainly focuses on environmentally friendly lead-free perovskites solar cells.

Zhao-Kui Wang received his Ph.D. degree in Nano and Novel Matter Science at University of Toyama, Japan, in 2011. After working at the University of Toyama as a JSPS research fellow from 2011 to 2013, he joined the Institute of Functional Nano & Soft Materials (FUNSOM), Soochow University, as an associate professor. Since 2017, he has been a full professor at Soochow University. His main research interest lies in organic and inorganic/organic hybrid materials and devices, focusing on solar cells and light-emitting diodes.